Clinical & Experimental Immunology
The Journal of Translational Immunology

Clinical and Experimental Immunology ORIGINAL ARTICLE doi:10.1111/j.1365-2249.2012.04652.x

Bead-size directed distribution of *Pseudomonas aeruginosa* results in distinct inflammatory response in a mouse model of chronic lung infection

L. J. Christophersen,* H. Trøstrup,*
D. S. Malling Damlund,*
T. Bjarnsholt,* K. Thomsen,*
P. Ø. Jensen,* H. P. Hougen,†
N. Høiby* and C. Moser*
*Department of Clinical Microbiology 93.01, Copenhagen University Hospital, Rigshospitalet, and †Department of Forensic Medicine, University of Copenhagen, Copenhagen, Denmark

Summary

Chronic *Pseudomonas aeruginosa* lung infection in cystic fibrosis (CF) patients is characterized by biofilms, tolerant to antibiotics and host responses. Instead, immune responses contribute to the tissue damage. However, this may depend on localization of infection in the upper conductive or in the peripheral respiratory zone. To study this we produced two distinct sizes of small alginate beads (SB) and large beads (LB) containing *P. aeruginosa*. In total, 175 BALB/c mice were infected with either SB or LB. At day 1 the quantitative bacteriology was higher in the SB group compared to the LB group ($P < 0{\cdot}003$). For all time-points smaller biofilms were identified by Alcian blue staining in the SB group ($P < 0{\cdot}003$). Similarly, the area of the airways in which biofilms were identified were smaller ($P < 0{\cdot}0001$). A shift from exclusively endobronchial to both parenchymal and endobronchial localization of inflammation from day 1 to days 2/3 ($P < 0{\cdot}05$), as well as a faster resolution of inflammation at days 5/6, was observed in the SB group ($P < 0{\cdot}03$). Finally, both the polymorphonuclear neutrophil leucocyte (PMN) mobilizer granulocyte colony-stimulating factor (G-CSF) and chemoattractant macrophage inflammatory protein-2 (MIP-2) were increased at day 1 in the SB group ($P < 0{\cdot}0001$). In conclusion, we have established a model enabling studies of host responses in different pulmonary zones. An effective recognition of and a more pronounced host response to infection in the peripheral zones, indicating that increased lung damage was demonstrated. Therefore, treatment of the chronic *P. aeruginosa* lung infection should be directed primarily at the peripheral lung zone by combined intravenous and inhalation antibiotic treatment.

Keywords: animal models/studies – mice/rats, cystic fibrosis (CF), cytokines/interleukins, lung immunology/disease

Accepted for publication 13 July 2012
Correspondence: C. Moser, Department of Clinical Microbiology 93.01, Copenhagen University Hospital, Rigshospitalet, Juliane Mariesvej 22, Copenhagen 2100-DK, Denmark.
E-mail: moser@dadlnet.dk

Introduction

Most patients with the inherited disease cystic fibrosis (CF) acquire a chronic lung infection with *Pseudomonas aeruginosa*. Once chronic *P. aeruginosa* lung infection is established it is almost impossible to eradicate, despite relevant antibiotic treatment and substantial innate and adaptive host responses. The background for the tolerance of the chronic *P. aeruginosa* lung infection to antibiotics and host responses is the formation of biofilms, where the bacteria are organized in micro colonies surrounded by an extracellular matrix. Because the infection remains in the lungs, continuous induction of pulmonary inflammation and stimulation of the adaptive immune response is the result. In fact, both parts of the host immune response contribute to the lung pathophysiology. The constantly recruited polymorphonuclear neutrophil leucocytes (PMNs) contribute by release of exoproteases, reactive oxygen and nitrogen species, and the induced T helper type 2 (Th2)-dominated response contributes by induction of a pronounced antibody response resulting in immune complex disease [1].

The activation and recruitment of the host response is, however, not uniform throughout the lung. The upper part of the lungs (trachea, bronchi and bronchioles), physiologically termed the conductive zones, are important for humidification and air warming, as well as for capture of inhaled particles and microbes. In the normal functioning lung, those captured elements are transported to the

oropharynx by the mucociliary escalator from where they are swallowed or cleared by coughing. In CF the cilia function is impaired severely due to dehydration of the airway surface liquid (ASL), and the particles and microbes are stuck in the larger airways within the ASL [2].

Microbes within the mucus can be aspirated to the lower or more peripheral parts of the airways – physiologically termed the respiratory zone (respiratory bronchioles and alveoli). Besides being the zone where gas exchange takes place, this part of the lung harbours the alveolar macrophages, type II alveolar epithelial cells and the majority of the pulmonary dendritic cells (DCs). Primarily the alveolar macrophages, but also type II alveolar cells, recognize the pathogen-associated molecular patterns (PAMPS; e.g. peptidoglycan, lipopolysaccharide, flagella) of the aspirated microbes by their pathogen-recognizing receptors (PRRs) [3,4]. The PRRs include the Toll-like receptors (TLRs) and nucleotide-binding oligomerization domaine (NOD)-like receptors (NLRs) and activation of the PRRs initiates the host response, resulting in release of cytokines [3,4]. Furthermore, the respiratory zones of the lung are in close contact with blood supply, as the total blood volume pumped from the right cardiac ventricle passes through the capillaries of the respiratory zone and back to the left cardiac ventricle as oxygenated blood [5]. Due to close contact between the alveolar space and the vascular lumen, this is also the major focus for recruitment of inflammatory cells through the endothelium, basal membrane and alveolar epithelium into the alveolar lumen [3,4]. The mechanism involves the mobilization of inflammatory cells from the bone marrow, up-regulation of blood cell integrins and selectins and endothelium adhesion molecules, as well as dilatation and leaking of capillaries to allow humoral and cellular components to pass into the pulmonary lumen and the invading microbes. In contrast, the blood to the upper conductive zone is limited to the arterial blood supply, comprising only 1% of the total cardiac output [5]. Despite the presence of a submucosal plexus, recruitment of inflammation to the conductive zone is relatively limited, probably because of the thicker tissue wall, the mucus produced by the goblet cells and the submucosal glands and the non-phlogistic s-immunoglobulin (IgA) in contrast to the phlogistic IgG response in the respiratory zone [6,7].

The majority of animal models applied for studying chronic *P. aeruginosa* lung infection is based on the embedding of bacteria in beads consisting of agar, agarose or seaweed alginate to prevent rapid clearance of the bacteria from the lungs. Therefore, we speculated whether improved control of the size, when producing *P. aeruginosa*-containing beads, would enable us to investigate the contribution of the two pulmonary zones to infection-induced inflammation (i.e. small beads in the respiratory zone *versus* large beads in the conductive zone), as distinct sizes of bacteria-containing beads should induce distinct inflammatory responses.

To investigate this hypothesis further we used an Encapsulation Unit Nisco Var J30 (NISCO Engineering AG, Zurich, Switzerland), which enables production of distinct sizes of *P. aeruginosa* containing seaweed alginate beads, through variation of nozzle size, air pressure and alginate flow rate. The aim of the present study was to study the course of chronic *P. aeruginosa* in groups of mice challenged with large or small *P. aeruginosa*-containing beads.

Materials and methods

Encapsulation Unit Nisco Var J30

The alginate enters through a central needle. The exit nozzle, which is centrally in line with the axis of the needle, has been countersunk externally, leading to the aerodynamic effect so that the jet has a smaller diameter when passing the nozzle than before at the needle. The needle is enclosed in a pressure chamber with an exit through the orifice. The size of the drop is determined by the nozzle size, the product flow rate and the pressure inside the chamber. The product flow rate is controlled by a syringe pump to be connected to the product nozzle. The pressure chamber is controlled by the pressure-controlling unit. The pressure set point is fixed with a potentiometer.

Bacterial strain

The clinical isolate *P. aeruginosa* strain PAO579 was propagated from a freeze culture for 18 h and grown for 18 h at 37°C in Ox-broth (Statens Serum Institute, Copenhagen, Denmark). The overnight culture was centrifuged at 4°C and 4400 ***g*** and the pellet resuspended in 5 ml serum-bouillon (KMA Herlev Hospital, Herlev, Denmark).

Beads preparation

Protanal LF 10/60 (FMC BioPolymer N-3002 Drammen, Norway) was dissolved in 0·9% NaCl to an alginate concentration of 1% and sterile filtered. The bacterial culture was diluted 1:20 in seaweed alginate solution. The solution was transferred to a 10-ml syringe and placed into a syringe pump (Graseby 3100; Ardus Medical Inc., Watford, UK). The syringe pump controls and feeds the alginate to the Encapsulation Unit Nisco Var J30. The J30 uses a pressure chamber containing a needle that controls the flow of alginate. The pressure chamber is controlled by the pressure controlling unit. The pressure set point is fixed with a potentiometer. The J30 unit is equipped with two connections, one for the alginate and one for the airflow that drives the alginate from the needle through the exit orifice into a gelleting bath (0·1 M, pH 7·0 Tris HCL buffer containing 0·1 M $CaCl_2$). A magnetic stirrer (IKA RCT Basic; IKA®-Werke GmbH & Co. KG, Staufen, Germany) is placed underneath the gelling bath to prevent the beads from sticking together during gelling.

The distance between nozzle and gelling bath of 11 cm and 280 rpm magnetic stirrer were kept constant. Five ml of alginate beads were made. The beds were left for stabilization at magnetic stirring in the gelleting bath for 1 h; the beads were then washed twice in 0·9% NaCl containing 0·1 M $CaCl_2$. After washing, 20 ml 0·9% NaCl containing $CaCl_2$ were added.

Determining the *P. aeruginosa* concentration

To determine the number of bacteria in the alginate beads the beads were dissolved to release the bacteria using 0·1 M citric acid buffer pH 5. Serial dilutions were made and cultured on a modified Conradi-Drigalski medium (SSI), selective for Gram-negative rods. After overnight incubation at 37°C the number of colony-forming units (CFU) was determined. The concentrations of *P. aeruginosa* in both the small beads (SB) and large beads (LB) varied from 0·2 to 0·7 CFU/ml; in no experiment did the concentration of bacteria in the beads differ more than 19%, and the bacterial concentration was lowest in the SB in all experiments.

Measuring bead sizes

In the present work we made beads in two different sizes. For the SB we used the 0·250 mm nozzle, an alginate flow rate 20 ml/h and the airflow 105 mBar. For the LB the 0·500 nozzle, alginate flow rate 60 ml/h and airflow 35 mBar were used. The diameter of the beads were measured using a light microscope (Olympus, Tokyo, Japan) and a picture-analysing program (Visiopharm Image Analysis and Stereology, Alleroed, Denmark). Two diameters at right angles were determined for each bead and presented as the mean.

Mouse strain

Female 11-week-old BALB/c mice were purchased from Taconic Europe A/S (Lille Skensved, Denmark) and allowed to acclimatize for 1 week before use. A total of 207 mice were used in the experiments. Mice had free access to chow and water, and were under the observation of trained personnel. All experiments were authorized by the National Animal Ethics Committee, Denmark.

Challenge procedure

Mice were anaesthetized subcutaneously (s.c.) with a 1:1 mixture of etomidate (Janssen, Birkeroed, Denmark) and midazolam (Roche, Basel, Switzerland) (10 ml/kg body weight) and tracheotomized. SB or LB seaweed alginate beads embedded with PAO579 were installed into the left lung of BALB/c mice using a bead-tipped needle. All mice received the same amount of alginate and number of *P. aeruginosa* ($0{\cdot}66 \times 10^9$ CFU/ml for the SB group *versus* $0{\cdot}71 \times 10^9$ CFU/ml for the LB group). An additional 32 mice were challenged with beads prepared as described but without adding *P. aeruginosa* to the alginate.

Mice were killed using an overdose of barbiturate at days 1, 2, 3, 5 or 6 after challenge. Peripheral blood was collected by cardiac puncture and serum isolated after centrifugation of coagulated blood. Serum was kept at −70°C until analysis. Half the number of lungs were collected aseptically and transferred to 5 ml of sterile phosphate-buffered saline (PBS) and kept on ice until further analysis. The left lungs from the remaining number of mice were fixed in a 4% w/v formaldehyde solution (VWR, Copenhagen, Denmark).

Histopathology

Evaluation of pulmonary histopathology was performed as described previously [8]. The fixed lungs were embedded in paraffin wax and cut into 5-µm-thick sections, followed by haematoxylin and eosin or Alcian blue staining. The entire lung slide was scanned at a low magnitude and, from an average evaluation of a minimum of five representative areas at higher magnitude (×400 or ×1000), the type and degree of lung inflammation was estimated. The type of inflammation was categorized as acute type (>90% PMNs), chronic type [>90% mononuclear cells (MNs)], both types present, neither dominating (PMN/MN) or no inflammation (NI). The degree of inflammation was scored on a scale from 0 to 3+, where 0 = no inflammation, + = mild focal inflammation, ++ = moderate to severe focal inflammation and +++ = severe inflammation to necrosis, or severe inflammation throughout the lung. Finally, the localization of the inflammation in the airway lumen or parenchyma was noted.

Alcian blue staining was used to identify airways containing alginate. The whole left lung was examined and airways which stained blue were noted and the area of the lumen estimated. In addition, the number and area of biofilms that stained blue were noted.

Peptide nucleic acid (PNA)–fluorescence *in-situ* hybridization (FISH)

To confirm the nature of the biofilm-like structures in the airways, deparaffinized tissue sections were analysed by FISH using PNA probes. A mixture of Texas Red-labelled, *P. aeruginosa*-specific PNA probe and fluorescein isothiocyanate (FITC)-labelled, universal bacterium PNA probe in hybridization solution (AdvanDx, Inc., Woburn, MA, USA) was added to each section and hybridized in a PNA–FISH workstation at 55°C for 90 min covered by a lid. The slides were washed for 30 min at 55°C in wash solution (AdvanDx). Vectashield mounting medium with 4′, 6-diamidino-2-phenylindole (DAPI) (Vector Laboratories, Burlingame, CA, USA) was applied, and a coverslip was added to each slide. Slides were read using a fluorescence microscope equipped with FITC, Texas Red and DAPI filters.

Quantitative bacteriology

Lungs for quantitative bacteriology were prepared as described previously [9]. In brief, lungs were removed aseptically and homogenized in 5 ml of PBS and serial dilutions of the homogenate were plated, incubated for 24 h and numbers of CFU were determined and presented as log CFU per lung.

Cytokine production

The lung homogenates were centrifuged at 4400 ***g*** for 10 min and the supernatants isolated and kept at −70°C until cytokine analysis. The concentrations in the lung homogenates of the PMN chemoattractant and murine interleukin (IL)-8 analogue macrophage inflammatory protein-2 (MIP-2) and of the PMN mobilizer granulocyte colony-stimulating factor (G-CSF) as well as the concentration of G-CSF in serum were measured by enzyme-linked immunosorbent assay (ELISA) (R&D Systems, Minneapolis, MN, USA), according to the manufacturer's instructions.

Statistical analysis

The number of mice in each group was calculated to provide a power of 0·80 or higher for continuous data. Statistical calculations were performed using EXCEL (Microsoft Office Line, Seattle, WA, USA). The χ^2 test was used when comparing qualitative variables and the analysis of variance (ANOVA)/unpaired *t*-test was used when comparing quantitative variables. $P \leq 0{\cdot}05$ was considered statistically significant (two-tailed tests).

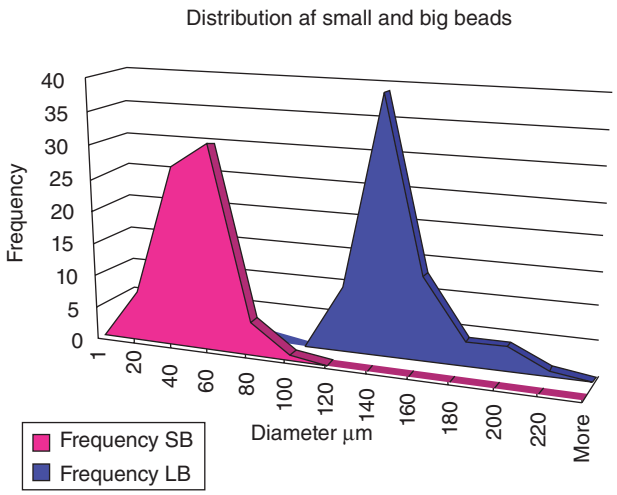

Fig. 1. Size distribution of seaweed alginate beads. Different sizes of *Pseudomonas aeruginosa* containing seaweed alginate beads were produced using different nozzle size, airway pressure and volume speed of alginate. Mean value of two diameters measured at right angles for each bead ($n = 72$). Two distinct populations of beads were produced.

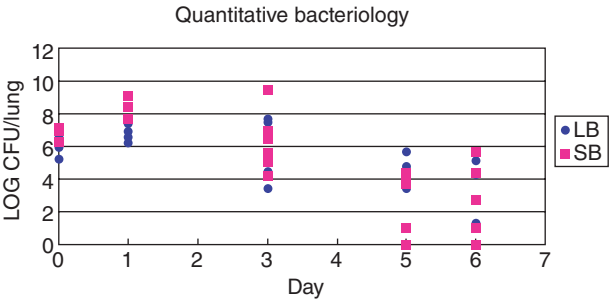

Fig. 2. Number of *Pseudomonas aeruginosa* in the lungs of BALB/c mice infected with two different sizes of *P. aeruginosa* containing seaweed alginate beads. All mice received the same number of bacteria and the same amount of alginate in the left lung. The number of colony-forming units (CFU)/ml was significantly higher at day 1 after infection in the group of mice infected with the small beads (SB). At other time-points, no significant difference in quantitative bacteriology could be observed.

Results

Distinct bead sizes

Diameters were determined for $n = 72$ beads and were 136 µm (range 74–205 µm) for LB and 40 µm (range 15–85 µm) for SB (Fig. 1a). Using the formula for sphere volume = $4/3 \times \pi \times r^3$, the LB were found to have a mean volume of 1 317 000 µm^3 compared to 34 000 µm^3 for the SB, giving a ratio difference in volume of 38·7 between LB and SB. Using the formula for sphere surface area = $4 \times p \times r^2$, the LB were found to have a surface area of 58 107 mm^2 compared to 5027 mm^2 for the SB, giving a ratio difference in surface area of 11·6 between LB and SB. Because both groups received the same amount of bacteria and alginate, this provides a larger total surface area of the SB of 3·3 (38·7/11·6 = 3·3). In addition, the volume of alginate in the two bead suspensions was adjusted to ensure equal volumes of alginate in the two groups.

Quantitative bacteriology

At day 1 after challenge, a significantly higher number of CFUs was observed in the lungs of SB group compared to the LB group ($P < 0{\cdot}003$) (Fig. 2). At days 3, 5 and 6 no significant differences in quantitative bacteriology were observed between the two groups. *P. aeruginosa* could be cultured from the majority of mice at all time-points (Fig. 2). Four mice from each group were killed 2 h after infection, and lungs examined for number of CFUs to confirm that the infection dose was equal in the two groups. No significant differences were observed in CFUs 2 h after challenge (Fig. 2).

Histopathology

As expected, a PMN-dominated inflammation was observed in all mice at day 1 after infection (Table 1). However, in the

Table 1. Evaluation of type and degree of inflammation in the two groups of BALB/c mice infected with different sizes of *Pseudomonas aeruginosa* containing seaweed alginate beads. At day 1, the inflammation was located endobronchially exclusively in the small beads (SB) group, whereas a mixed localization of inflammation was observed in the large beads (LB) group. In the SB group the inflammation shifted significantly to a mixed localization at days 2/3 after infection ($P < 0{\cdot}01$); haematoxylin and eosin staining.

	Large beads			Small beads		
	Inflammation		Parenchyma/bronchia	Inflammation		Parenchyma/bronchia
Days after infection	Type	Degree	(endoluminal)	Type	Degree	(endoluminal)
Day 1 ($n = 8$)	4 PMN	0+++	0 Parenchyma	4 PMN	0+++	0 Parenchyma
	0 PMN/MN	4++	3 Bronchia	0 PMN/MN	4++	4 Bronchia
	0 MN	0+	1 Parenchyma and bronchia	0 MN	0+	0 Parenchyma and bronchia
	0 NI	0 NI		0 NI	0 NI	
Days 2/3 ($n = 10$)	3 PMN	3+++***	1 Parenchyma	2 PMN	3+++***	0 Parenchyma
	2 PMN/MN	2++	0 Bronchia	2 PMN/MN	1++	0 Bronchia
	0 MN	0+	4 Parenchyma and bronchia	0 MN	0+	4 Parenchyma and bronchia*
	0 NI	0 NI		1 NI	1 NI	
Days 5/6 ($n = 16$)	0 PMN	2+++	2 Parenchyma	1 PMN	2+++	0 Parenchyma
	5 PMN/MN	1++	0 Bronchia	2 PMN/MN	1++	0 Bronchia
	0 MN	2+	3 Parenchyma and bronchia	0 MN	0+	3 Parenchyma and bronchia
	3 NI	3 NI		5 NI	5 NI**	

*A significant change from endobronchial localization exclusively to a mixed localization of inflammation at days 2/3 in the SB group ($P < 0{\cdot}005$). **A significantly faster resolution of inflammation in the SB group compared to the LB group ($P < 0{\cdot}03$). ***Both groups showed a significant increase in degree of inflammation from day 1 to days 2/3 ($P < 0{\cdot}01$). MN: mononuclear cells; NI: no inflammation; PMN: polymorphonuclear lymphocytes.

SB group the inflammation was located exclusively endobronchially, in contrast to a partially mixed localization in the LB group (Table 1). In the SB group this shifted significantly to a mixed localization or exclusively parenchymal localization on days 2/3 after challenge ($P < 0{\cdot}005$, Table 1), and in general was paralleled by a more peripheral presence of the bacteria in the alveoli of the SB group. For the SB group, a significantly faster resolution of inflammation at days 5/6 compared to the LB group was observed ($P < 0{\cdot}03$, Table 1). For both groups together, a significant increase in degree of inflammation from day 1 to days 2/3 was observed ($P < 0{\cdot}01$, Table 1). However, the difference between the two groups for this observation did not reach significance.

Area of biofilm-like structures and airways

The area of the biofilm-like structures identified by Alcian blue staining were significantly smaller in the SB group compared to the LB group at day 1 and days 2/3 ($P < 0{\cdot}001$, Figs 3 and 4). In accordance, the area of the airways in which biofilm-like structures were identified were significantly smaller in the SB group compared to the LB group at days 2/3 ($P < 0{\cdot}002$, Figs 3 and 4). The number of identified biofilm-like structures was 137 in the LB group *versus* 308 in the SB group. PNA-FISH and DAPI staining confirmed the presence of *P. aeruginosa* in the biofilm-like structures (Fig. 5).

Cytokines

In serum, the concentrations of the PMN mobilizer G-CSF were increased significantly at day 1 after challenge in the SB group compared to the LB group ($P < 0{\cdot}0001$, Fig. 6). At days 3, 5 and 6 no significant differences were observed between the groups (Fig. 6). A similar pattern was observed in the supernatants from the lung homogenates, with significantly increased G-CSF in the SB group at day 1 ($P < 0{\cdot}0001$) but no significant differences at other time-points (Fig. 7). In accordance, in the supernatants of the lung homogenates the concentrations of the PMN chemoattractant MIP-2 were increased significantly at day 1 after challenge in the SB groups compared to the LB group ($P < 0{\cdot}0001$, Fig. 8). At days 3, 5 and 6 no significant differences were observed (Fig. 8). Cytokines measured in serum and homogenates from mice challenged with sterile beads were negligible at all time-points compared to mice challenged with *P. aeruginosa*-containing beads ($P < 0{\cdot}01$; Figs 6–8).

Discussion

Lungs are constantly exposed to inhaled or aspirated pathogens, allergens and irritants. However, the distribution of such elements in the lungs is highly variable. The upper airways are colonized with bacteria from the oropharynx, whereas the lower normal airways are sterile. In recent years increasing attention has been drawn to the significance of the different zones in the lungs, in relation to concentration of gases [10,11], to induction and recruitment of inflammation and to severity of tissue damage [12] and presence of bacteria [7]. The present study demonstrates how different sizes of infectious beads can result in different inflammatory responses due to different localization of the infectious beads, as a correlation was observed between infection with small beads, localization of smaller

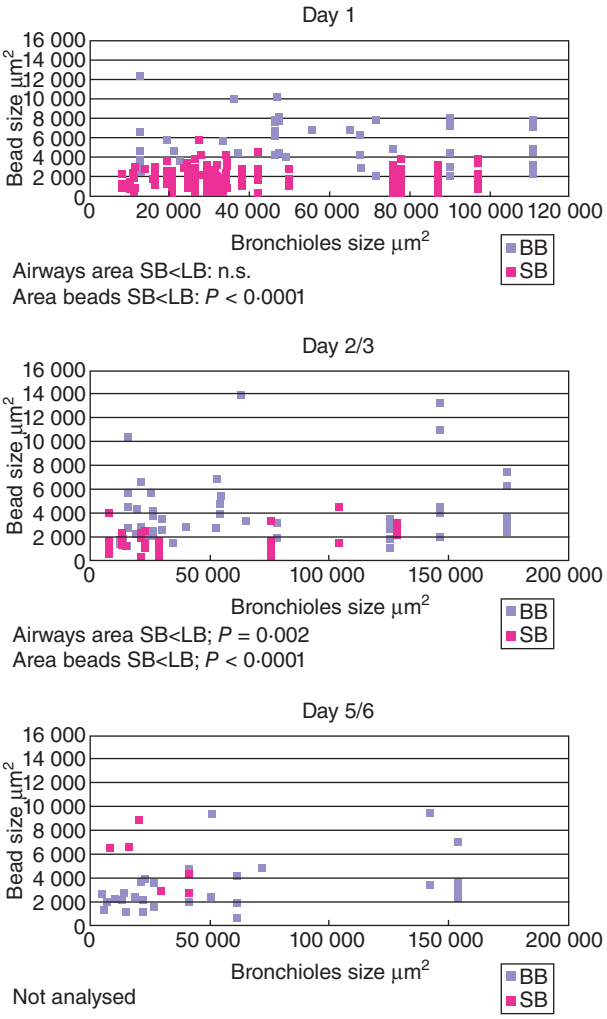

Fig. 3. The distribution and sizes of *Pseudomonas aeruginosa*-containing seaweed alginate beads was estimated after Alcian blue staining. At all time-points smaller beads were identified in the small beads (SB) challenge group ($P < 0{\cdot}0001$), although statistical analysis could not be performed for days 5/6 due to too few identifiable beads and representative bronchioles in the SB group. At days 2/3 the beads were identified in significantly smaller airways of the BALB/c mice lungs infected with the SB ($P < 0{\cdot}002$). The same trend was observed at day 1, but did not reach statistical significance.

biofilm-like structures in smaller airways and an increased inflammatory response.

During the continuous dichotomized division from trachea to the two main bronchi to the respiratory bronchioles, the total trans-sectional area of the airways is increased gradually; however, the trans-sectional area of the individual airway is reduced gradually. As a consequence, larger particles are captured primarily in the upper airways whereas smaller particles can proceed all the way to the alveoli. From previous studies on deposits of particles in the lungs it would have been optimal with even smaller beads below 10 μm in diameter [13]. However, trying to make smaller beads with a smaller nozzle was not possible due to clotting of the small nozzle. Furthermore, studies on localization of particles in the lungs have been performed on inhalation through nose and/or mouth, whereas our challenge procedure was through a tracheotomia. In addition, our beads were forced through a needle into the left main bronchus with a syringe providing a certain pressure, which may lead to a more peripheral localization of the beads.

Even using this artificial exposure procedure, we observed different localizations in the airways of the two distinct bead sizes, suggesting that localization of the infection can be controlled by bead size. In the mice infected with SB, infection and inflammation could be seen all the way to the periphery of the lungs next to the pleural membrane. In a recent study, using the traditional bead preparation providing a mean size beads of 60 μm, comparing mucoid and non-mucoid isotypes of *P. aeruginosa*, only the mucoid isolates had the ability to proceed to the very periphery of the lungs [14]. However, with the new procedure in bead preparation employed in the present study and using a

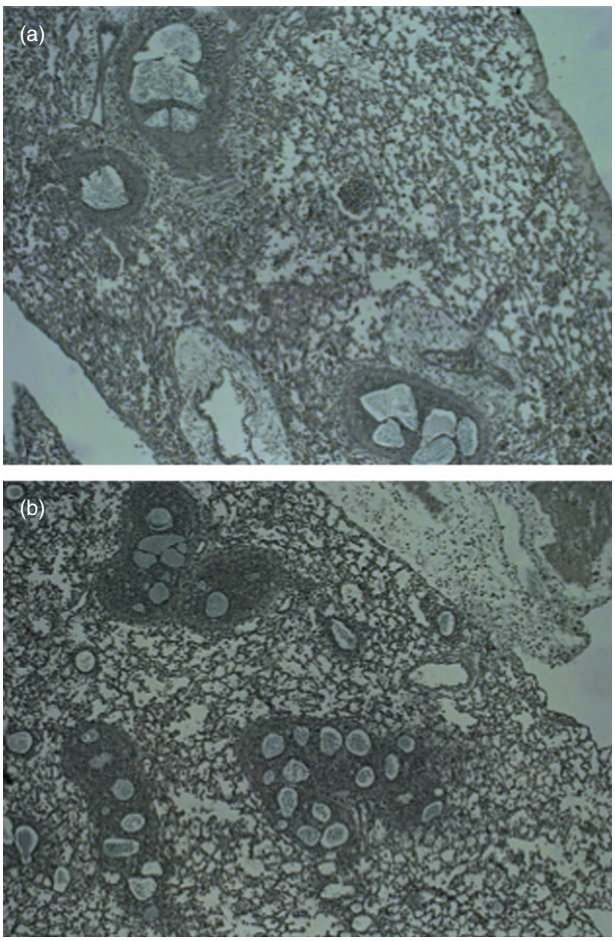

Fig. 4. Alcian blue staining of lung slides prepared from mouse lungs obtained at day 1 after infection with either large beads (LB) in (a) and small beads (SB) in (b). Alcian blue staining was performed to identify the biofilm-like alginate-containing structures in the lungs. Magnification ×400.

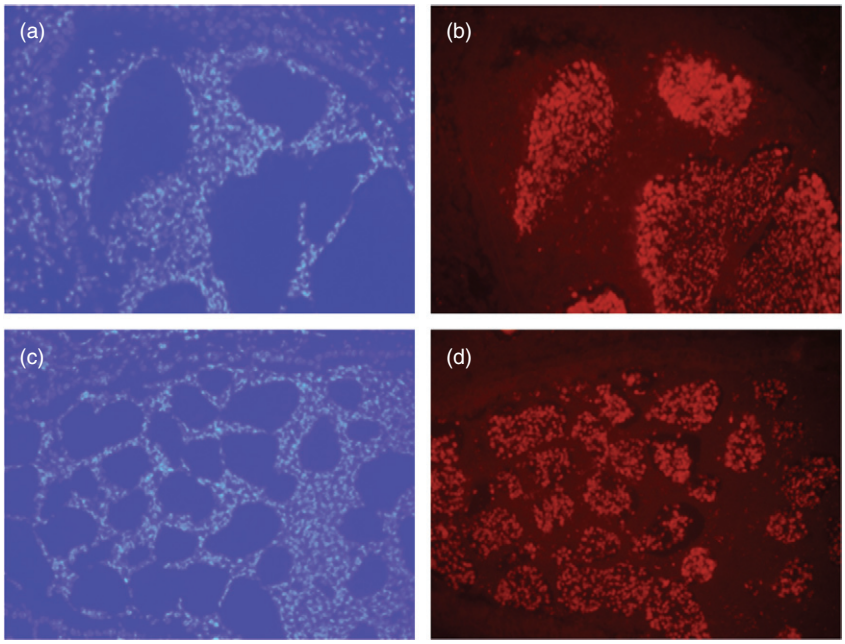

Fig. 5. The presence of *Pseudomonas aeruginosa* in the biofilm-like structures in the airways of BALB/c mice was confirmed by specific peptide nucleic acid–fluorescence *in-situ* hybridization (PNA–FISH) technique staining *P. aeruginosa* red. PMNs are stained blue by 4′, 6-diamidino-2-phenylindole (DAPI). (a) (LB) and (c) (SB) show DAPI-stained lungs and (b) (LB) and (d) (SB) the corresponding PNA–FISH-stained lungs obtained at day 1 after infection with *P. aeruginosa*-containing alginate beads. All magnification ×400.

non-mucoid isolate, bacteria in the small beads could be identified in the alveoli of the lungs.

Localization of pathogens in the lungs is of particular interest with respect to inflammation. In the larger airways pathogens are caught primarily in the s-IgA-containing mucus and transported by the mucociliary escalator to the mouth without initiating inflammation. In addition, the ability to initiate inflammation in the larger airways is limited, as immunological cells are not located in the epithelial tissue of larger normal airways except for scanty lymphoid cells and specialized DCs. Recruitment of inflammation in the larger airways is also impaired due to limited blood supply and the distance from vascular lumen to airway lumen. In addition, the dominating class of antibodies in the upper airways is the non-opsonizing and complement non-activating secretory IgA secreted from the submucosal lymphoid aggregates in the conducting zones [6,15].

Similarly, the involvement of intraepithelial conventional CD11b^{-} DCs (cDCs), lamina propia CD11B^{high} cDCs and plasmacytoid (pDCs) without danger signals add to this anti-inflammatory state of the immune system [16]. As the

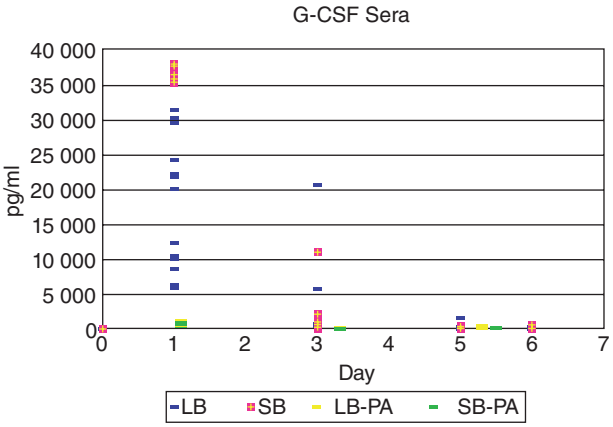

Fig. 6. Serum were obtained from all mice by cardiac puncture. Concentrations of the polymorphonuclear leucocytes (PMN) mobilizer granulocyte colony-stimulating factor (G-CSF) were determined by enzyme-linked immunosorbent assay (ELISA). G-CSF concentrations were increased significantly in the small beads (SB) group compared to the large beads (LB) group at day 1 ($P < 0{\cdot}0001$). No statistically significant differences were observed at other time-points.

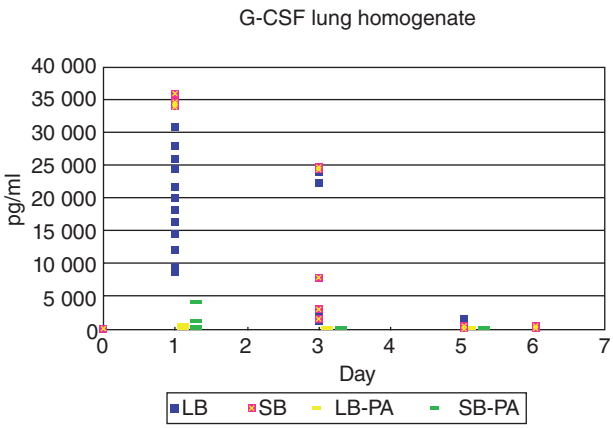

Fig. 7. Concentrations of the polymorphonuclear leucocytes (PMN) mobilizer granulocyte colony-stimulating factor (G-CSF) in the supernatants of the lung homogenates were determined by enzyme-linked immunosorbent assay (ELISA). G-CSF concentrations were increased significantly in the small beads (SB) group at day 1 compared to the large beads (LB) group ($P < 0{\cdot}0001$). No statistically significant differences were observed at other time-points.

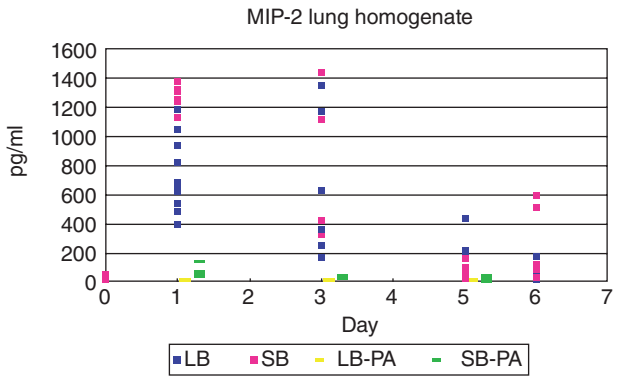

Fig. 8. Concentrations of the polymorphonuclear leucocytes (PMN) chemoattractant macrophage inflammatory protein-2 (MIP-2) in the supernatants of the lung homogenates were determined by enzyme-linked immunosorbent assay (ELISA). MIP-2 concentrations were increased significantly in the small beads (SB) group at day 1 compared to the large beads (LB) group ($P < 0{\cdot}0001$). No statistically significant differences were observed at other time-points.

upper airways are significantly more exposed to intruders than the lower airways, this is a suitable arrangement to avoid constant irritation and inflammation of the upper airways.

In contrast, professional immune cells, especially alveolar macrophages and supported by type II epithelial cells, are located in the alveoli and with their PRRs they can rapidly recognize the PAMPs of pathogens being inhaled or aspirated to the periphery of the lungs [3,4,16,17]. The initiated inflammation follows within few hours, primarily with recruitment of PMNs, and influx of humoral factors such as complement, defensins and cytokines, as the alveolar lumen and vascular lumen is within a distance of a few μm. In chronic infection, IgG synthesized in the medulla of the regional lymph nodes and the bone marrow, and induced by different subsets of $CD11B^{high}$ and $CD11B^{-}$ cDCs and pDCs induced by danger signals via the alveolar macrophages and type II alveolar epithelial cells, will also be present in the airway lumen resulting in opsonin activation of PMNs and complement activation, thereby further enhancing inflammation [6,7,15,16,17].

However, the problematic consequence of the strong inflammatory response in the alveoli is loss of the major functional tissue of the lungs, namely the lung niches where gas exchange takes place. Therefore, pathogen-induced inflammation to those areas is much more critical than localization in the larger airways except, of course, for the risk of aspiration to the smaller airways. In accordance, our results demonstrated a significantly higher degree of inflammation in the lung challenges with the smaller beads, as demonstrated by increased pulmonary concentration of the PMN chemoattractant MIP-2 and increased serum concentration of the PMN mobilizer from the bone marrow G-CSF. In this regard, we speculate that the reduction of serum G-CSF observed after elective intravenous (i.v.) antibiotic treatment of chronically infected CF patients [18] is caused by an attenuation of bacteria in the respiratory zone of the lungs.

An interesting observation, however, was that after the initial reduced clearance of the smaller beads and the subsequent increased inflammation, bacteria in both small and large beads were already equally cleared at days 2/3. Our interpretation is that the stronger inflammatory response in combination with the total of 3·3 larger total surface of the smaller beads made the latter easier to clear; however, never to a significantly lower level compared to the large beads.

In relation to the CF patients, the clinical consequence of the present observations may be that it is of pivotal importance that the given antibiotics are directed primarily at the smaller airways, as this is where the inflammation is induced and where the most important tissue damage takes place. In treatment this is obtained i.v. due to the high perfusion of the alveoli and the short diffusion distance into and inside the alveoli [19–21]. Inhalation antibiotics reach the alveoli to a much smaller extent, but reach the microbes in the larger airways at very high concentrations, and may also prevent microbes from being aspirated to previously uninfected niches of the lungs.

In conclusion, the present study demonstrates that pulmonary inflammation is highly dependent on distribution of the pathogens in the lungs. Because inflammation is increased significantly by pathogens in the peripheral lung parts, these physiologically important respiratory zones are more likely to be damaged by induced inflammation, especially during chronic infections as seen in CF.

Disclosure

No relevant disclosures.

References

1 Jensen PO, Givskov M, Bjarnsholt T, Moser C. The immune system vs. *Pseudomonas aeruginosa* biofilms. FEMS Immunol Med Microbiol 2010; **59**:292–305.

2 Knowles MR, Boucher RC. Mucus clearance as a primary innate defense mechanism for mammalian airways. J Clin Invest 2002; **109**:571–7.

3 Craig A, Mai J, Cai S, Jeyaseelan S. Neutrophil recruitment to the lungs during bacterial pneumonia. Infect Immun 2009; **77**:568–75.

4 Schmiedl A, Kerber-Momot T, Munder A, Pabst R, Tschernig T. Bacterial distribution in lung parenchyma early after pulmonary infection with *Pseudomonas aeruginosa*. Cell Tissue Res 2010; **342**:67–73.

5 McCullagh A, Rosenthal M, Wanner A, Hurtado A, Padley S, Bush A. The bronchial circulation – worth a closer look: a review of the relationship between the bronchial vasculature and airway inflammation. Pediatr Pulmonol 2010; **45**:1–13.

6 Pedersen SS, Moller H, Espersen F, Sorensen CH, Jensen T, Høiby N. Mucosal immunity to *Pseudomonas aeruginosa* alginate in cystic fibrosis. APMIS 1992; **100**:326–34.

7 Bjarnsholt T, Jensen PO, Fiandaca MJ *et al*. *Pseudomonas aeruginosa* biofilms in the respiratory tract of cystic fibrosis patients. Pediatr Pulmonol 2009; **44**:547–58.

8 Moser C, PØ J, Kobayashi O *et al*. Improved outcome of chronic *Pseudomonas aeruginosa* lung infection is associated with induction of a Th1-dominated cytokine response. Clin Exp Immunol 2002; **127**:206–13.

9 Moser C, Johansen HK, Song Z, Hougen HP, Rygaard J, Høiby N. Chronic *Pseudomonas aeruginosa* lung infection is more severe in Th2 responding BALB/c mice compared to Th1 responding C3H/HeN mice. APMIS 1997; **105**:838–42.

10 Wörlitzsch D, Tarran R, Ulrich M *et al*. Effects of reduced mucus oxygen concentration in airway *Pseudomonas* infections of cystic fibrosis patients. J Clin Invest 2002; **109**:317–25.

11 Kolpen M, Hansen CR, Bjarnsholt T *et al*. Polymorphonuclear leucocytes consume oxygen in sputum from chronic *Pseudomonas aeruginosa* pneumonia in cystic fibrosis. Thorax 2010; **65**:57–62.

12 Lee B, Schjerling CK, Kirkby N *et al*. Mucoid *Pseudomonas aeruginosa* isolates maintain the biofilm formation capacity and the gene expression profiles during the chronic lung infection of CF patients. APMIS 2011; **119**:263–74.

13 West JB. Pulmonary physiology and pathophysiology. An integrated case-based approach. Philadelphia, PA: Lippincott Williams & Wilkins, 2001.

14 Moser C, Van Gennip M, Bjarnsholt T *et al*. Novel experimental *Pseudomonas aeruginosa* lung infection model mimicking long-term host-pathogen interactions in cystic fibrosis. APMIS 2009; **117**:95–107.

15 Janeway CA. Immunobiology. Garland Sci 2011; **6** (Part IV): Chapter 9.

16 Plantinga M, Hammad H, Lambrecht BN. Origin and functional specializations of DC subsets in the lung. Eur J Immunol 2010; **40**:2112–8.

17 Rohmann K, Tschernig T, Pabst R, Goldmann T, Dromann D. Innate immunity in the human lung: pathogen recognition and lung disease. Cell Tissue Res 2011; **343**:167–74.

18 Jensen PO, Moser C, Kharazmi A, Presler T, Koch C, Hoiby N. Increased serum concentration of G-CSF in cystic fibrosis patients with chronic *Pseudomonas aeruginosa* pneumonia. J Cyst Fibros 2006; **5**:145–51.

19 Høiby N, Ciofu O, Bjarnsholt T. *Pseudomonas aeruginosa* biofilms in cystic fibrosis. Future Microbiol 2010; **5**:1663–74.

20 Thiberville L, Moreno-Swirc S, Vercauteren T, Peltier E, Cave C, Bourg Heckly G. *In vivo* imaging of the bronchial wall microstructure using fibered confocal fluorescence microscopy. Am J Respir Crit Care Med 2007; **175**:22–31.

21 Høiby N. Recent advances in the treatment of *Pseudomonas aeruginosa* infections in cystic fibrosis. BMC Med 2011; **9**: 32 (pp. 1–7).